Measurement of polymeric time scales from linear drop oscillations

Gregor Plohl*, Günter Brenn
Institute of Fluid Mechanics and Heat Transfer, Graz University of Technology, Austria
*Corresponding author: gregor.plohl@tugraz.at

Abstract

The oscillating drop method allows material properties of liquids to be measured from damped drop oscillations. The literature discusses, e.g., the measurement of the liquid dynamic viscosity and the surface tension against the ambient medium, predominantly for Newtonian liquids. We use this method for measuring pairs of material properties of polymeric liquids. Pairs of properties may be measured, since the quantity measured is a complex frequency with a real and an imaginary part. For the measurements, individual drops are levitated in air by an ultrasonic levitator and imaged with a high-speed camera. Amplitude modulation of the ultrasound drives shape oscillations of the levitated drop. When the modulation is switched off, with the levitating force maintained, the drop performs free oscillations which are damped due to the liquid viscosity. The data acquired from the images recorded are the angular frequency and the damping rate which are used as an input into the characteristic equation of the oscillating drop. Our measurements intend to yield either two viscoelastic time scales with the zero-shear viscosity known, or one time scale and the zero-shear viscosity, with the other time scale known. The two time scales are the stress relaxation and the deformation retardation times. The latter is difficult to get for polymer solutions.

The present contribution presents results from a large set of measurements of the deformation retardation time. Liquids studied are aqueous solutions of poly(acryl-amides) at varying concentration. The corresponding values of the zero-shear viscosity agree well with the values from shear rheometry. Values of the deformation retardation time differ substantially from the values commonly used in viscoelastic flow simulations. Furthermore, the measured values disagree with the predictions from the viscous-elastic stress splitting approach in linear viscoelasticity. With our study we will provide a consistent set of material properties for the Oldroyd-B model in linear viscoelasticity. This will be important for material modelling in viscoelastic spray simulations.

Keywords

Linear drop shape oscillations, damped oscillations, polymeric liquid, ultrasonic levitation.

Introduction

The deformations of a drop surface due to shape oscillations may influence transport processes across the liquid/gas interface, such as the evaporation of the drop or the absorption of gases from the environment. For their relevance for transport processes, and for scientific interest, oscillations of liquid drops have been under investigation since the time of Lord Rayleigh, who derived the angular frequency $\alpha_{m,0} = \sqrt{m(m-1)(m+2)}\sqrt{\sigma/\rho a^3}$ of linear oscillations of mode m for an inviscid drop with density ρ, radius a, and surface tension σ against the ambient vacuum [1]. Rayleigh's work was extended by Lamb [2], who included the influence of viscosity of the drop liquid and obtained the oscillation frequency and the rate of decay of the oscillations in the limits of very high and very low drop viscosity.

The idea to measure material properties of liquids from damped drop shape oscillations has brought about the oscillating drop method [3, 4]. To date, the existing literature discusses the measurement of material parameters, such as the dynamic viscosity of the liquid and its surface tension against the ambient medium, predominantly for Newtonian liquids [5-8].

For viscoelastic systems, the oscillating drop method was used for investigating the surface rheology [9, 10]. The materials were surfactant solutions, and the drops were levitated due to the microgravity conditions of the experiment. In these studies, complementary effects of the bulk and the surface viscosities were found [9] and quantified [10]. Most recently, the oscillating drop method was proposed and developed for measuring polymeric time scales [11-13]. The basis of the method is the characteristic equation for the complex frequency of the drop. The experiments were carried out with aqueous solutions of the two different poly(acryl-amides) Praestol 2500 and Praestol 2540 with different degree of hydrolysis and hence different mechanical flexibilities of the macromolecules. The drops were levitated using an ultrasonic levitator. The aim of the first study [11] was to quantify the influences of the two polymeric time scales on the oscillation behavior of the drop, and to propose an experimental method to determine the deformation retardation time by measuring damped oscillations of the drop. A proof-of-concept experiment was

presented to show the potential and limitations of the method. In [12], the characteristic equation was further analyzed, and a numerical method for determining a pair of liquid properties from the characteristic equation was presented. The method was tested for three different aqueous polymer solutions (0.3 and 0.8 wt.% Praestol 2500 and 0.05 wt.% Praestol 2540). The values of the deformation retardation time λ_2 obtained by this method deviate strongly from the values typically used in viscoelastic flow simulations. The sensitivity and uncertainty analysis have shown the values of λ_2 depend weakly on the uncertainty of the experimental data.

In the present study, the oscillating drop method [11-13] was used to study the deformation retardation time dependency on the polymer concentration. We have studied aqueous solutions of Praestol 2500 with polymer mass fractions between 0.1 and 1.0 wt.%. Our paper is organized as follows: first the theoretical foundations of drop shape oscillations are presented. We then outline the experiment for measuring the complex oscillation frequency. Further, we present and discuss the experimental results and draw the conclusions.

Theoretical Foundations

The equations governing linear viscoelastic drop shape oscillations are the equation of continuity $\boldsymbol{\nabla} \cdot \boldsymbol{v} = 0$ and the linearized equation of motion

$$\rho \frac{\partial \boldsymbol{v}}{\partial t} = -\boldsymbol{\nabla} \cdot (p\boldsymbol{\delta} - \boldsymbol{\tau}) \tag{1}$$

The extra stress tensor $\boldsymbol{\tau}$ is related to the flow field through the appropriate linear viscoelastic material model. Material models in fluids relate rates of deformation to the extra stresses, which appear on top of some isotropic stress, such as pressure. Material models follow either from micro-rheological or from phenomenological approaches. The former consists in a transport equation for the dyadic of the end-to-end position vector of the macromolecules with itself, which yields information about the state of deformation of the molecules in the solution and, thereby, about the stress. The phenomenological approach models extra stresses and their changes by a transport equation. The rheological equations of state representing the material model must satisfy invariance criteria in coordinate transformations and must be independent of the motion of the material as a whole [14].

The most general form of a phenomenological material model for a viscoelastic fluid is the Oldroyd eight-constant model [15]. It allows non-linear material behavior to be modelled and relies on the eight constant parameters of the model, which all have the dimension of time, except the dynamic viscosity involved. Simplifying this model to the linear case, i.e., treating a liquid as linear viscoelastic, the extra stress in the liquid at small rates of deformation may be described by the differential equation

$$\boldsymbol{\tau} + \lambda_1 \frac{d\boldsymbol{\tau}}{dt} = -\eta_0 (\dot{\boldsymbol{\gamma}} + \lambda_2 \frac{d\dot{\boldsymbol{\gamma}}}{dt}) \tag{2}$$

where λ_1 and λ_2 are the stress relaxation and deformation retardation times, η_0 is the zero shear viscosity and $\dot{\gamma}$ is the rate of deformation tensor. This equation is also known as the *Jeffreys* model. The relaxation time characterizes the time scale on which the stress relaxes after removal of strain, and the retardation time describes the strain relaxation after removal of stress. The case $\lambda_1 = \lambda_2 = 0$ describes the purely viscous Newtonian fluid, and the case $\lambda_2 = 0$, $\lambda_1 > 0$ describes the purely elastic fluid. With the time dependency of motion given by an exponential function *exp*$(-\alpha_m t)$, where α_m is the complex angular frequency of mode *m*, the stress tensor τ satisfying Eq.(2) reads

$$\boldsymbol{\tau} = \eta_0 \frac{1 - \alpha_m \lambda_2}{1 - \alpha_m \lambda_1} \dot{\boldsymbol{\gamma}} = \eta(\alpha_m)\dot{\boldsymbol{\gamma}} \tag{3}$$

This equation indicates that the linear viscoelastic extra stress may be represented formally in the same way as for a Newtonian fluid, with the difference that the dynamic viscosity $\eta(\alpha_m)$ depends on the complex frequency α_m (correspondence principle). In our discussions on the linear stability behaviour of viscoelastic liquid systems below we will assume material behaviour according to this model. Shear thinning, as a non-linear phenomenon, is therefore not accounted for, which is strictly correct for Boger fluids, but neglects some potentially important phenomenon in shear thinning liquids. In the latter case, however, linear liquid behaviour on the first Newtonian plateau of the flow curve may still be represented correctly by the linear approach [16].

In polymer science and in computational rheology, it is customary to decompose the stress into its Newtonian and non-Newtonian components (referred to as the *viscous-elastic stress splitting*) or, more generally, to write the extra stress $\boldsymbol{\tau} = \boldsymbol{\tau}_s + \boldsymbol{\tau}_p$ and the dynamic viscosity $\eta_0 = \eta_s + \eta_p$ as sums of contributions from the Newtonian solvent and the polymer (*solvent-polymer stress splitting*) [17, 18]. A similar approach can be applied also for the Giesekus model [19]. This approach yields the Jeffreys model (Oldroyd B) if the deformation retardation time is defined as

$$\lambda_2 = \lambda_1 \frac{\eta_s}{\eta_s + \eta_p} = \lambda_1 \frac{\eta_s}{\eta_0} =: \lambda_{2G} \tag{4}$$

The damped oscillatory motion of the drop is analyzed in detail in [11, 12]. The fundamental outcome of the analysis is the characteristic equation for the complex frequency of the drop

$$\left(\frac{\alpha_{m,0}}{\alpha_m}\right)^2 = \frac{2(m^2 - 1)}{q^2 a^2 - 2qa j_{m+1}/j_m} - 1 + \frac{2m(m-1)}{q^2 a^2}\left[1 + \frac{2(m+1)j_{m+1}/j_m}{2qa j_{m+1}/j_m - qa}\right] \tag{5}$$

where $q = \sqrt{\alpha_m/\nu(\alpha_m)}$ and j_m and j_{m+1} are spherical Bessel functions of the first kind at the value qa of their arguments. The equation is formally identical to the results of Lamb [2] obtained for Newtonian liquids. In the present case of a viscoelastic liquid, however, the kinematic viscosity involved in the equation is a function of the complex oscillation frequency α_m. The equation is transcendental in qa and must therefore be solved numerically to determine, e.g., the zero-shear dynamic viscosity η_0 and the deformation retardation time λ_2 involved in the dynamic viscosity $\eta(\alpha_m) = \nu(\alpha_m)\rho = \eta_0(1 - \alpha_m\lambda_2)/(1 - \alpha_m\lambda_1)$. Knowing the real and imaginary parts of the complex oscillation frequency α_m from the experiment, we get two pieces of information from the characteristic equation. In the following section we present an experiment suitable for measuring the complex oscillation frequency α_2 of the drop.

Experimental method

The experiment bases on the levitation of an individual drop in a standing ultrasound wave [20]. The acoustic resonator consists of a transducer and a curved reflector allowing for the stable placement of a drop with a diameter ≤ 3 mm (Fig. 1). Liquids studied are aqueous solutions of poly(acryl-amides) at varying concentration. The drops are produced and placed into the acoustic field with an insulin syringe (Fig. 2 left, center). Oscillation frequencies excited by ultrasound modulation are $O(120$ Hz$)$, close to the resonance frequency of the base-mode m=2. After switch-off of the modulation, the drop returns to its equilibrium shape by damped oscillations (Fig. 2 right).
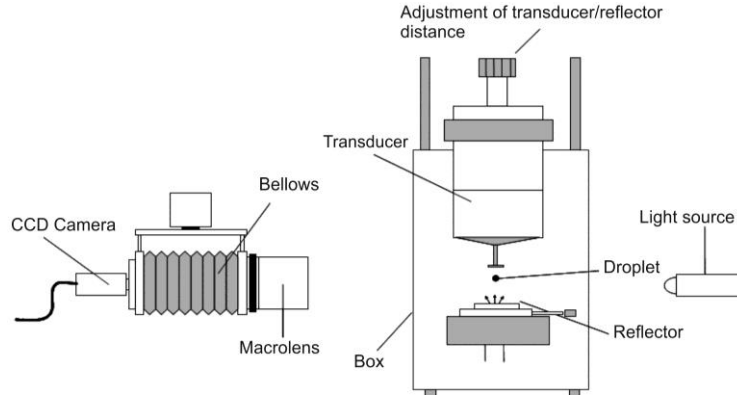

Figure 1. Experimental setup with acoustic levitator for drop shape oscillation studies.
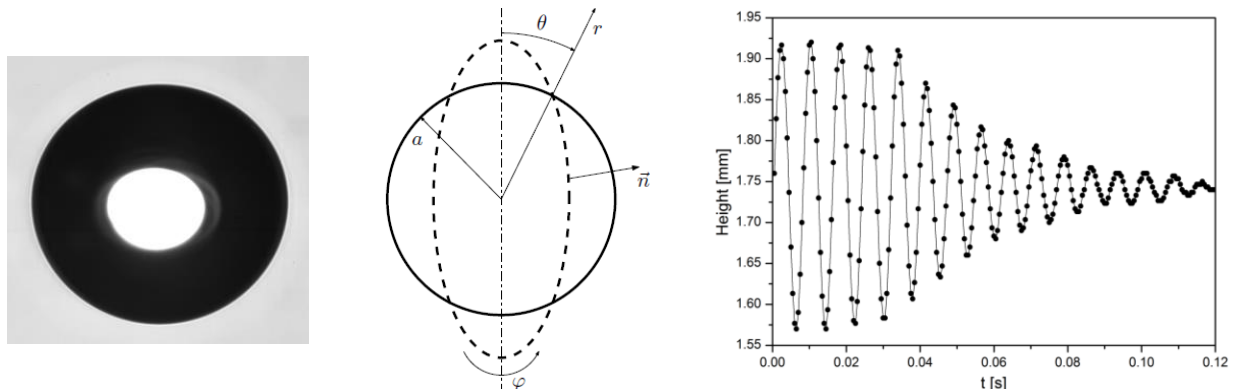

Figure 2. (Left) Shape of a levitated 1.7 mm drop, (center) equilibrium and deformed drop shapes in the spherical coordinate system. The deformed shape (dashed line) is represented by $r_s(\theta, t) = a + \epsilon_0 P_m(\cos\theta)\exp(-\alpha_m t)$ [11], (right) distance between the north and south poles in a damped drop oscillation as a function of time.

The data acquired from the high-speed camera recording of the damped oscillations are the angular frequency $\alpha_{m,i}$ and the damping rate $\alpha_{m,r}$. For determining the pair of liquid properties (η_0, λ_2), the two values $\alpha_{m,i}$ and $\alpha_{m,r}$ are used as an input into the characteristic equation (5) of the drop, so that the left-hand side of the equation is known.

Our experiments were carried out with aqueous solutions of the poly(acryl-amide) Praestol 2500 from Solenis Technologies (Germany). This is a non-ionic polymer with a degree of hydrolysis of 3 – 4% and molecular weight about 15-20 $\cdot 10^6$ kg/kmol. The aqueous solutions were prepared in demineralized water, producing a master solution with a solute mass fraction of 10000 ppm by mass, which was then diluted to achieve the various mass fractions. The shear viscosity of the liquids was measured as a function of shear rate with a rotational rheometer Anton Paar MCR 300. The values of the zero-shear viscosity η_0^* (first Newtonian plateau) were determined from measured flow curves approximated by the empirical Carreau-Yasuda model. The temperature was kept constant at the value of 22°C ± 1°C in the laboratory where the drop oscillation experiments were carried out. The densities of the liquids were measured with an oscillating U-tube device with an accuracy of ±0.1 kg/m^3. They are all in the order of 10^3 kg/m^3. The surface tension of the liquids against the ambient air was measured with a drop volume tensiometer. The stress relaxation time λ_1 of the liquids was measured with a filament stretching elongational rheometer yielding mean values with standard deviations between 6 and 15% [20]. The properties of the aqueous solutions of the poly(acryl-amide) Praestol 2500 investigated in the present study are listed in Table 1 and presented in Fig. 3.

Table 1. Properties of the aqueous Praestol 2500 polymer solutions at 22°C.

| Solute mass fraction w [$wt.\%$]	Density ρ [$kg\ m^{-3}$]	Surface tension σ [$N\ m^{-1}$]	Zero-shear viscosity η_0* [$Pa\ s$]	Stress relaxation time λ_1 [s]
0.1	1000	0.0722	0.013 ± 10%	0.025 ± 10%
0.2	1000	0.0727	0.033 ± 10%	0.066 ± 10%
0.3	1000	0.0732	0.08 ± 10%	0.11 ± 10%
0.4	1000	0.0737	0.12 ± 10%	0.12 ± 10%
0.5	1000	0.0743	0.39 ± 10%	0.16 ± 10%
0.6	1000	0.0748	0.56 ± 10%	0.18 ± 10%
0.7	1000	0.0753	0.9 ± 10%	0.21 ± 10%
0.8	1000	0.0758	1.6 ± 10%	0.23 ± 10%
0.9	1000	0.0763	2.3 ± 10%	0.25 ± 10%
1.0	1000	0.0769	3.9 ± 10%	0.285 ± 10%
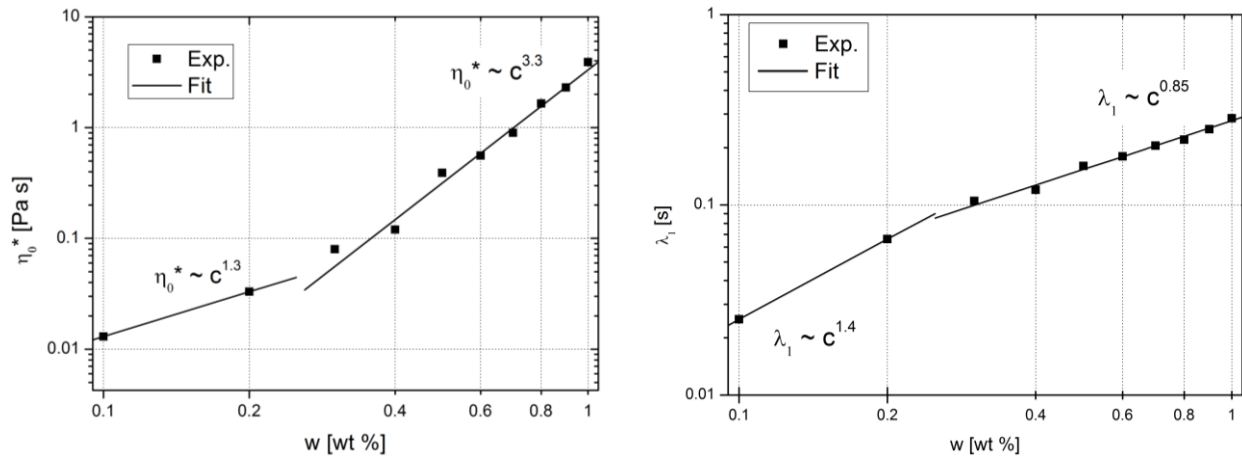
Figure 3. Praestol 2500 aqueous solutions. (Left) Zero-shear viscosity and (right) relaxation time against polymer mass fraction.

Figure 3 (left) shows the zero-shear viscosity against polymer mass fraction. The measured data are approximated by the scaling law

$$\eta_0 \propto w^S \tag{6}$$

where $S \approx 1.3$ at low polymer mass fractions w, and $S \approx 3.3$ for high polymer mass fraction. The transition between these two regimes lies between w=0.2 and 0.3 wt.% (Fig. 3 left). Figure 3 (right) shows the dependence of the

relaxation time on the polymer mass fraction w. The measured values are approximated using the similar scaling law $\lambda_1 \propto w^T$, where $T \approx 1.4$ for low concentrations and $T \approx 0.85$ for higher concentrations. The transition between these two regimes lies again between w=0.2 and 0.3 wt.%. The region between 0.3 and 1.0 wt.% can be seen as a semi-dilute regime, and the region between 0.1 and 0.2 wt.% as the transition from the dilute to the semi-dilute regime.

Images of the levitated drop are recorded by a high-speed camera at a framing rate of 2 *kHz* under backlight illumination. An uncertainty in the length measurement of ±2 *Pxls* with the resolution of 300 *Pxls/mm* results in a sizing uncertainty of ±6.7 *µm*, which is equivalent to ±0.3% for a 2 *mm* drop. Within at most 10 *s* after the drop has been placed in the acoustic levitator, several pictures of the drop are taken in order to have its initial shape and volume. This initial state, where the evaporation of the solvent has had no influence on the solution concentration yet, allows the concentration of the drop liquid at all later times to be deduced from the volume. The equilibrium radius a is calculated from the recorded instantaneous images. The zero-shear viscosity obtained from the experiment is the value corresponding to the concentration of the solution present during the related experiment.

The experiment for determining the polymeric deformation retardation time from damped drop oscillations is subject to influences from the experimental method of acoustic levitation and the non-Newtonian behavior of the polymeric liquid, which is shear-thinning in many cases. In order to fulfill the limitations set by the linear theory underlying the characteristic equation of the drop, and in order to avoid influences from the shear thinning of the liquid, we measure the drop oscillation frequency and damping rate in the late stages of the damped oscillation.

The oscillation shown in Figure 2 (right) was recorded for a 0.3 wt.% Praestol 2500 solution drop with the equilibrium diameter of 1.83 *mm*. The drop was driven at 130 *Hz* before the modulation was switched off. From these data, the frequency and damping rate in the last part of the motion were extracted, so that both the linear oscillation behavior was ensured and the shear-thinning of the polymer solution did not have any influence on the oscillation. The frequency and damping rate are determined using the least-squares method to achieve the best fit of a prescribed function to the damped oscillations measurement data. The fitting procedure was done of both oscillating directions, as shown in Figure 4 (left) and the average value for the frequency and the damping rate were calculated. The volume-equivalent spherical radius was also calculated (Figure 4 right) and compared to initial radius in order to determine the correct polymer concentration.

The angular frequency and the damping rate of the drop depicted in Fig. 2, determined by this procedure, are $\alpha_{2,i} = (2\pi) \cdot 134.2$ *Hz* and $\alpha_{2,r} = 36.2$ *s*$^{-1}$. The real and imaginary parts of the complex angular frequency $\alpha_2 = \alpha_{2,r} + i\alpha_{2,i}$ are therefore known.
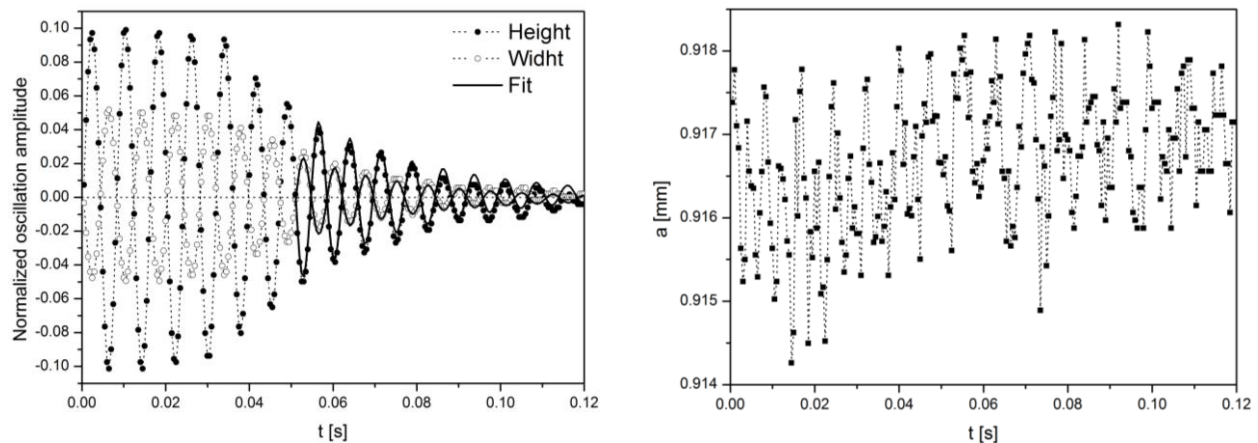

Figure 4. Damped oscillations of a levitated 1.72 mm 0.3 wt% aqueous Praestol 2500 solution drop as a function of time. (Left) Normalized oscillation amplitude and the fitting curve (solid line) in the last part of the motion. (Right) Volume-equivalent spherical radius of the drop as a function of time, varying by no more than 0.3%.

Solutions of the characteristic equation

The characteristic equation (5) is transcendental in the argument of the spherical Bessel functions involved and must therefore be solved numerically. The method for determining η_0 and λ_2 by solving this equation and the detailed analysis of the characteristic equation are presented in [12]. For the numerical analysis we use the computer algebra software MATHEMATICA. As a prerequisite, the complex frequency α_m must be accurately measured in the experiment, and the radius of the drop as well as the density, surface tension and stress relaxation time of the liquid in contact with the ambient air must be known. Due to the influence from the spherical Bessel functions, the equation

exhibits a complicated set of solutions. Identification of the right solution among the calculated pairs of η_0 and λ_2 follows from comparison of the value of η_0 with the result η_0^* from the measurements with a rotational viscosimeter. The solutions qa of the characteristic equation and corresponding calculated values of zero shear viscosity η_0 and deformation retardation time λ_2 for a 0.3 wt% aqueous Praestol 2500 solution drop are listed in Table 2.

Table 2. Positive roots *qa* of the characteristic equation and corresponding calculated values of zero shear viscosity η_0 and deformation retardation time λ_2 for the 0.3 wt% Praestol 2500 solution drop in Fig. 3. The correct solution is highlighted.

Radius [*mm*]	Frequency [*Hz*]	Damping rate [*s*$^{-1}$]	qa	η_0 [*Pa·s*]	λ_2 [*s*]
0.917	134.2	36.2	4.385 + 7.8312*i*	0.0002	2130·10^{-4}
± 0.006	± 0.4	± 2.5	4.974 + 0.0791*i*	2.656	1.267 ·10^{-4}
			8.767 + 0.0426*i*	0.856	1.005·10^{-4}
			12.116 + 0.0263*i*	0.448	0.941·10^{-4}
			15.363 + 0.0164*i*	0.279	0.915·10^{-4}
			18.569 + 0.0106*i*	0.191	0.903·10^{-4}
			21.755 + 0.0071*i*	0.139	0.897·10^{-4}
			24.928 + 0.0049*i*	0.106	0.894·10^{-4}
			28.093 + 0.0036*i*	**0.083**	**0.893·10^{-4}**
			31.254 + 0.0027*i*	0.067	0.892·10^{-4}
			34.411 + 0.0020*i*	0.056	0.891·10^{-4}
			37.564 + 0.0016*i*	0.047	0.891·10^{-4}

From the error analysis [12] follows that λ_2 can be accurately determined even if the right solution qa cannot unambiguously be identified. This is due to the weak dependency of λ_2 on the solution qa of the characteristic equation. This weak dependency is demonstrated in Table 2. On the other hand, in order to accurately determine η_0, very accurate measurements of all the input parameters are required.

Results and discussion

With each of the ten polymer solutions we performed a set of about 35 measurements in order to get statistically reliable results. From each polymer solution, five drops with different radius were levitated and with each of these drops, we performed 6 to 8 oscillation measurements. The results are presented in Table 3 and in Fig. 5. Table 3 shows the set of viscosities and deformation retardation times of the aqueous polymer solutions (Table 1), where values obtained as solutions of the characteristic equation are compared to values of the deformation retardation time from the viscous-elastic stress splitting approach $\lambda_{2G} = \lambda_1 \eta_s / \eta_0^*$. The value of the solvent viscosity η_s used was 1 mPa s for water. The uncertainty of the values listed in Table 3 is of the order of 10%.

Table 3. The viscosities η_0 and deformation retardation times λ_2 obtained from oscillating drop measurements. For comparison the zero shear viscosity η_0^* and the deformation retardation λ_{2G} from the viscous-elastic stress splitting approach are also listed.

Solute mass fraction w [*wt%*]	Viscosity η_0 [*Pa s*]	Zero-shear viscosity η_0^* [*Pa s*]	Retardation time λ_2 [10^{-4} s]	Retardation time λ_{2G} with η_0^* [10^{-4} s]
0.1	0.013	0.013	0.35	19.23
0.2	0.037	0.033	0.47	20.00
0.3	0.08	0.08	0.9	13.75
0.4	0.127	0.12	2	10.00
0.5	0.43	0.39	2.1	4.10
0.6	0.51	0.56	2.5	3.21
0.7	0.82	0.9	2.7	2.33
0.8	1.65	1.6	2.9	1.38
0.9	2	2.3	3.1	1.09
1.0	6	3.9	3.5	0.73
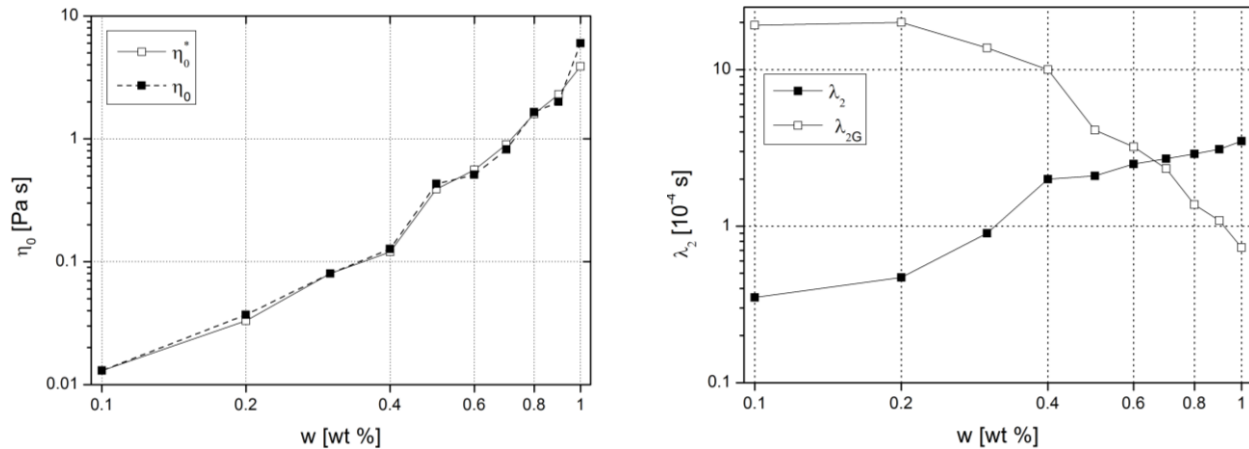
Figure 5. (Left) Calculated η_0 and measured η_0^* and (right) λ_2 and λ_{2G} against Praestol 2500 polymer mass fraction *w*.

Zero shear viscosity

The values of the zero-shear dynamic viscosity agree with the values from the shear viscosimetry to within ±10%, except for the 1.0 wt.% polymer solution. This disagreement could be due to experimental error, i.e. the measurement error of the input parameters is too large. A second reason for the disagreement could be that this case may be close to the limit of applicability of our method regarding the polymer concentration, since we must keep in mind that our experimental method relies on the ability of the drop to perform damped periodic oscillations. Once the drop Ohnesorge number threshold to aperiodic behavior is exceeded, the deformed drop returns to its equilibrium state in an aperiodic manner, so that our method cannot be applied any more. This will be the subject of further studies.

Deformation retardation time

The results show that the measured deformation retardation time λ_2 increases monotonically with the polymer mass fraction *w*. For the concentrations studied, values of λ_2 between 35 and 350 μs are obtained. On the other hand, λ_{2G} as defined by the viscous-elastic stress splitting approach decreases with increasing polymer mass fraction in the range of polymer mass fractions above *w*=0.2 wt.%. The two trends are equal only in the range of polymer mass fractions below 0.2 wt.%. The trend of λ_{2G} to vary with the polymer concentration is quantified as $(\partial\lambda_{2G}/\partial c)/\lambda_{2G} = (\partial\lambda_1/\partial c)/\lambda_1 - (\partial\eta_0/\partial c)/\eta_0$. With the dependencies of λ_1 and η_0 on the polymer concentration given above, we arrive at the condition that $(\partial\lambda_{2G}/\partial c)/\lambda_{2G}$ is positive only when T>S, which is the case in the sufficiently dilute regime below *w*=0.2 wt.% only. We conclude from this that the calculation of λ_2 with the viscous-elastic stress splitting approach reproduces the trend from the experiment correctly only in this sufficiently dilute regime, which corresponds to different polymer mass fraction regimes for different polymers and solvents. The absolute values of λ_{2G} obtained, however, still differ substantially from the result of the measurement. In the case of the present polymer solution, the measured values of λ_2 agree well with the calculated λ_{2G} for polymer mass fractions between 0.5 and 0.8 wt.% only, and this rather by coincidence. For the most dilute solutions studied, the measured and calculated values strongly deviate from each other, which finding remains to be explained once more polymer solutions were investigated. As one reason for these differences due to the different concentrations of the solutions we may see the fact that the more dilute solutions may be better described by the viscous-elastic stress splitting approach than the more concentrated solutions. This could indicate a limitation of the validity of the equation for λ_{2G} for concentrated systems. The absolute values of this time scale, however, still remain quite different even in the dilute solutions.

Conclusions

In this study we use linear damped shape oscillations of drops for measuring the zero-shear viscosity and the deformation retardation time of viscoelastic polymeric drop liquids. The solution of the linearized equations of change governing the drop shape oscillations yields the characteristic equation for the complex oscillation frequency which is used for determining the material properties. For a given drop, the oscillation frequency and the damping rate are measured in an experiment using acoustic levitation. Liquid material properties relevant for the oscillations, such as liquid density, surface tension and stress relaxation time, are measured by appropriate standard methods. The zero-shear viscosity and the deformation retardation time of the liquid are obtained as solutions of the characteristic equation of the oscillating drop. Values of the liquid dynamic viscosity are close to those from shear rheometry. They

allow the correct solution of the characteristic equation to be identified from a manifold and support the correctness of the deformation retardation times determined.

The values of λ_2 are found to deviate strongly from values often used in simulations of viscoelastic liquid flow. The values of λ_2 agree with λ_{2G} only for small region of polymer mass fractions (between 0.5 and 0.8 wt.%). Further work will be devoted to investigating the deformation retardation behaviour of various polymers at different concentrations in solvents of different quality.

Nomenclature

a	equilibrium drop radius [m]	$\alpha_m = \alpha_{m,r} + i\alpha_{m,i}$	complex angular frequency [s^{-1}]
j_m, j_{m+1}	spherical Bessel functions [1]	$\alpha_{m,0}$	inviscid angular frequency [s^{-1}]
m	mode number [1]	ε_0	oscillation amplitude [m]
p	pressure [Pa]	$\dot{\gamma}$	rate of deformation tensor [s^{-1}]
P_m	Legendre polynomials	η	dynamic viscosity [Pa s]
$q = q_r + iq_i$	complex inverse oscillatory length scale [m^{-1}]	η_0	zero-shear dynamic viscosity [Pa s]
r	radial coordinate	$\lambda_1, \lambda_2, \lambda_{2G}$	polymeric time scales [s]
S, T	scaling exponents [1]	ν	kinematic viscosity [m^2 s^{-1}]
t	time [s]	ρ	density [kg m^{-3}]
$\boldsymbol{v}$	velocity [m s^{-1}]	σ	surface tension [N m^{-1}]
w	polymer mass fraction [wt.%]	$\boldsymbol{\tau}$	extra stress tensor [Pa]

References

[1] Rayleigh, Lord, J.W.S., 1879, Proc. R. Soc. London A, 29, pp. 71-97.

[2] Lamb, H., 1881, Proc. London Math. Soc., 13, pp. 51-66.

[3] Kovalchuk, V., Krägel, J., Aksenenko, E., Loglio, G., Liggieri, L., 2001, in Möbius, D. & Miller, R. (Eds.): Novel methods to study interfacial layers, Elsevier Sci. B.V., pp. 485-516.

[4] Ravera, F., Loglio, G., Kovalchuk, V., 2010, Curr. Opin. Colloid Interface Sci., 15, pp. 217-228.

[5] Perez, M., Salvo, L. Suéry, M., Bréchet, Y., Papoular, M., 2000, Phys. Rev. E, 61, pp. 2669-2675.

[6] Egry, I., Lohöfer, G., Seyhan, I., Schneider, S., Feuerbacher, B., 1998, Appl. Phys. Lett., 73, pp. 462-463.

[7] Hiller, W.J., Kowalewski, T.A., 1989, Physico-Chem. Hydrodyn., 11, pp. 103-112.

[8] Hsu, C.J., Apfel, R.E., 1985, J. Colloid Interface Sci., 107, pp. 467-476.

[9] Tian, Y.R., Holt, R.G., Apfel, R.E., 1995, Phys. Fluids, 7, pp. 2938-2949.

[10] Apfel, R.E., Tian, Y.R., Jankovsky, J., Shi, T., Chen, X., Holt, R.G., Trinh, E., Croonquist, A., Thornton, K.C., Sacco, A. Jr., Coleman, C., Leslie, F.W., Matthiesen, D.H., 1997, Phys. Rev. Lett, 78, pp. 1912-1915.

[11] Brenn, G., Teichtmeister, S., 2013, J. Fluid Mech., 733, pp. 504-527.

[12] Brenn, G., Plohl, G., 2015, J. Non-Newton. Fluid Mech., 223, pp. 88-97.

[13] Yang, L., Kazmierski, B.K., Hoath, S.D., Jung, S., Hsiao, W.K., Wang, Y., Berson, A., Harlen, O., Kapur, N., Bain, C.D., 2014, Phys. Fluids, 26, 113103.

[14] Oldroyd, J., 1950, Proc. R. Soc. London A, 200, pp.523-541.

[15] Oldroyd, J., 1958, Proc. R. Soc. London A, 245, pp.278-297.

[16] Brenn, G., Plohl, G., 2017, Atomization Sprays, 27.

[17] Bird, R.B., Armstrong, R.C., Hassager, O., 1987, Dynamics of polymeric liquids. John Wiley, New York.

[18] Amoreira, L.J., Oliveira, P.J., 2010, Adv. Appl. Math. Mech., 2, pp. 483-502.

[19] Giesekus, H.W., 1994, Phänomenologische Rheologie – Eine Einführung (Phenomenlogical Rheology – An Introduction, in German), Springer, Berlin, Heidelberg, New York.

[20] Yarin, A.L., Brenn, G., Kastner, O., Rensink, D., Tropea, C., 1999, J. Fluid Mech., 399, pp. 151-204.

[21] Stelter, M., Brenn, G., Yarin, A.L., Singh, R.P., Durst, F., 2000, J. Rheology, 44, pp. 595-616.